Hindawi Publishing Corporation
International Journal of Corrosion
Volume 2015, Article ID 426397, 8 pages
http://dx.doi.org/10.1155/2015/426397

Research Article

Smart Mesoporous Silica Nanocapsules as Environmentally Friendly Anticorrosive Pigments

C. Zea,[1] R. Barranco-García,[1,2] B. Chico,[1] I. Díaz,[1] M. Morcillo,[1] and D. de la Fuente[1]

[1]*National Centre for Metallurgical Research (CENIM/CSIC), Avenida Gregorio del Amo 8, 28040 Madrid, Spain*
[2]*Institute of Polymer Science and Technology (ICTP/CSIC), C/Juan de la Cierva 3, 28006 Madrid, Spain*

Correspondence should be addressed to D. de la Fuente; delafuente@cenim.csic.es

Received 30 June 2015; Revised 28 August 2015; Accepted 30 August 2015

Academic Editor: Ramazan Solmaz

Nowadays there is a special interest to study and develop new smart anticorrosive pigments in order to increase the protection life time of organic coatings and, simultaneously, to find alternatives to conventional toxic and carcinogenic hexavalent chromium compounds. In this respect, the great development of nanotechnologies in recent years has opened up a range of possibilities in the field of anticorrosive paints through the integration of encapsulated nanoscale containers loaded with active components into coatings. By means of a suitable design of the capsule, the release of the encapsulated corrosion inhibitor can be triggered by different external or internal factors (pH change, mechanical damage, etc.) thus preventing spontaneous leakage of the active component and achieving more efficient and economical use of the inhibitor, which is only released upon demand in the affected area. In the present work, the improved anticorrosive behaviour achieved by encapsulated mesoporous silica nanocontainers filled with an environmentally friendly corrosion inhibitor has been evaluated. It has been proven that a change in the pH allows the rupture of the capsules, the release of the inhibitor, and the successful protection of the carbon steel substrate.

1. Introduction

The application of protective organic coatings is one of the most widespread approaches used nowadays for corrosion protection of different metallic materials. The main role of the anticorrosive coating is to protect metals forming effective barrier against corrosive species present in different environments. However, the aging of the polymer together with accidental mechanical impacts could lead to the formation of defects interrupting the barrier and providing direct ingress of the corrosive species to the metal surface [1]. After corrosion started, the polymer coating itself cannot protect the defective zone and is not able to stop propagation of the defect. For that reason, conventional anticorrosive paint coatings also contain pigments which constantly release substances actively inhibiting corrosion (corrosion inhibitors). However, this continuous and uncontrollable leaching of the active component could lead to fast exhausting and osmotic blistering of polymer films, both reducing the protection lifetime of the coating.

In addition, until recent years, anticorrosive paint formulation technologies have relied almost exclusively on the use of chromates as metallic corrosion inhibitor pigments. Different types of chromates (Cr^{6+}) have proven to be highly effective pigments in the protection of different metals against corrosion, especially in the case of steel. The great efficiency of organic coatings pigmented with chromates is attributed to three factors: (i) suitable solubility of chromate type pigments; (ii) high inhibitor efficiency; and (iii) establishment of a dynamic process of storage, release, transport, and inhibition [2]. However, the toxicity of these pigments to human health, given their carcinogenic effects [3], and to the environment [4, 5] is giving rise to severe restrictions on their use [6, 7].

All of this has spawned an exhaustive search for environmentally friendly alternatives to replace this type of anticorrosive pigments and has become the great challenge of the last years for all the sectors involved in anticorrosive protection by organic coatings. When it comes to designing and developing Cr^{6+}-free systems, it is necessary to take into

account all the factors that account for their efficiency. In other words, the effectiveness of the inhibitor in an organic coating requires not only efficiency to inhibit the corrosion process, but also the possibility of controlling its solubility and its release into the environment. To date, despite the great number of studies carried out worldwide and although some alternatives have shown good behaviour in certain conditions, no definitive solution has been found for the replacement of chromates by nontoxic pigments.

Recent developments in surface science and technology open up new opportunities through the integration of nanoscale containers (carriers) loaded with active components into coatings [8–12]. Suitable nanoparticle design would allow the controlled release of the inhibitor in response to external stimuli (change in pH, temperature, physical breakage of paint film, etc.), achieving a more efficient and economical use of the inhibitor, which is only released upon demand in the affected area [13–15].

One approach is to load active compounds into nanocontainers with a shell of controlled permeability and then to incorporate them into the coating matrix [8]. As a result, nanocontainers are uniformly distributed in the passive matrix keeping active material in a "trapped" state, thus avoiding the undesirable interaction between the active component and the passive matrix, leading to spontaneous leakage. Release from such a shell-like capsule is typically realized by its rupture and a prompt liberation of the carried substance. Meanwhile, a peak-like delivery is not necessarily desired because it centers the efficiency of delivery to one spot in time only. It is of technical interest to produce a shell-like capsule in which release is controlled by permeation through the shell material; however, it would be hard to ensure the mechanical stability of the coating as a whole, due to the eventual collapse of the capsule [16]. A prolongation in time delivery, so-called sustained release, can be achieved without the loss of mechanical stability when a porous particle instead of a shell-like capsule is used. Release of molecules stored in a porous matrix takes more time than those stored in a shell-like particle owing to the diffusion through the porous matrix [17]. Silica-based mesoporous particles are especially interesting as they retain their solid properties as long as pH of the surrounding medium is not exceeding ~11 [18].

In order to avoid spontaneous delivery, encapsulation of loaded mesoporous nanoparticles is also helpful [9]. Among the possible different technologies for encapsulation, the Layer-by-Layer (LbL) deposition technology of oppositely charged species (polyelectrolytes, nanoparticles, enzymes, dendrimers, etc.) represents an interesting approach to encapsulate inhibitor loaded reservoirs with regulated storage/release properties assembled with nanometer-thickness precision [13, 19, 20]. For example, LbL-assembled polyelectrolyte multilayers reveal controlled permeability properties. Depending on the nature of the assembled monolayers, the permeability of multilayer films can be controlled by changing pH, ionic strength, and temperature, or by applying magnetic or electromagnetic fields [21–25].

In the present work, SiO_2 mesoporous nanoparticles have been successfully synthesized, loaded with an environmentally friendly corrosion inhibitor and sodium phosphomolybdate, and encapsulated by the deposition of an oppositely charged polyelectrolyte. The morphology and porous structure of the nanoparticles have been characterized by FEG-SEM/EDX, TEM, and BET. The Z-potential of the different nanoparticles has been also measured. Regarding the anticorrosive behaviour, the loading and releasing capacity at different conditions has been determined and the inhibition capacity has been also obtained from polarization curves of carbon steel exposed to solutions of a different aggressiveness in presence of loaded nanoreservoirs.

2. Experimental Procedure

2.1. Synthesis of Monodisperse Mesoporous Silica Nanoparticles. Mesoporous silica spheres have been synthetized following the route described by Yamada and Yano [26]. In a typical synthesis, 1.68 g of *n*-dodecyl trimethylammonium bromide (C_{12}TMABr) as a surfactant and 3 mL of 1 M sodium hydroxide solution were dissolved in 400 g of ethylene glycol/water (25/75 = w/w) solution. Then 1.84 g of tetramethoxysilane (TMOS) was added to the solution, with vigorous stirring at 20°C. Following the addition of TMOS, the clear solution suddenly turned opaque, resulting in a white precipitate. After 8 h of continuous stirring the mixture was aged overnight. The solution was filtered in a vacuum assembly with a filter membrane (Durapore, Millipore, 0.10 μm pore size). After filtration, the white powder was washed with distilled water at least three times, then dried at 45°C for 6 h, and finally calcined in air in a muffle furnace at 550°C for 6 h in order to remove the organic template.

2.2. Loading of the Mesoporous Nanoparticles with Corrosion Inhibitor. Synthesized mesoporous silica nanoparticles were then loaded with sodium phosphomolybdate as corrosion inhibitor. To load the silica nanoparticles, 1 g of the synthetized mesoporous silica was added to 500 mL of 0.01 M $Mo_{12}Na_3O_{40}P$ solution. The pH of the sodium phosphomolybdate solution was adjusted to 2.3 in order to improve the loading, according to the results of a preliminary study. The suspension was kept under continuous stirring during 8 h and, then, the powder was filtered in a vacuum assembly with a filter membrane (Durapore, Millipore, 0.10 μm pore size) and washed with distilled water at least three times.

2.3. Encapsulation of the Loaded Nanoparticles. Loaded mesoporous silica nanoparticles were encapsulated by the application of a layer of a positively charged polyelectrolyte, poly(diallyldimethylammonium chloride) (PDDA). Initially, SiO_2 nanoparticles are negatively charged, so the adsorption of positive poly(diallyldimethylammonium chloride) (PDDA) is directly performed mixing, under stirring during 5 minutes, 1 g of the loaded silica with 250 mL of a 0.5 M NaCl and adding 3 mgmL^{-1} of PDDA. The resultant nanoparticles were filtered in a vacuum assembly with a filter membrane

(Durapore, Millipore, 0.10 μm pore size), washed with distilled water, and dried at 45°C for 2 h.

2.4. Characterization Study. The mesoporous silica nanoparticles, as-synthetized after calcination, loaded, and loaded/encapsulated, were observed and analyzed by means of a field emission scanning electron microscope with an Oxford Inca energy dispersion microanalysis system (FE-SEM/EDS, Hitachi S4800) and by means of a transmission electron microscope also equipped with energy dispersion microanalysis system (TEM/EDS, Philips Tecnai 20T). Before observation, the particles were dispersed in acetone in an ultrasonic bath for 5 min and then placed onto an iron grid in the case of SEM and onto a copper grid in the case of TEM.

The specific surface area and pore volume were obtained from N_2 adsorption-desorption isotherms at 77 K (Micromeritics TRISTAR 3000). The specific surface area was calculated from the adsorption data in the low pressure range ($0.05 \leq P/P^0 \leq 0.2$) by using the Brunauer-Emmett-Teller (BET) method. The average pore diameter and the pore volume were determined from the N_2 adsorption branch by the Barrett-Joyner-Halenda (BJH) method, defining the thickness of adsorbed N_2 layer by means of the Harkins and Jura equation.

The zeta potential (ζ-potential) of all produced silica nanoparticles, calcined, loaded, and loaded/encapsulated (10 mg silica/50 mL MilliQ water), was measured in triplicate in a Zetasizer nanoZ (Malvern instrument Ltd) at 25°C with the Smoluchowski approximation. Each value was obtained as an average from three runs of the instrument with at least 10 measurements.

2.5. Evaluation of pH-Dependent Corrosion Inhibitor Release. 50 mg of loaded/encapsulated mesoporous silica nanoparticles was added to 25 mL of aqueous solution at three different pH values (3, 6, and 11). The suspensions were kept under continuous stirring during 30 minutes and then filtered in a vacuum assembly with a filter membrane (Durapore, Millipore, 0.10 μm pore size). The Mo ion content in the aqueous extract was determined by inductively coupled plasma optical emission spectrometry (ICP-OES, PerkinElmer 4300 DV).

2.6. Electrochemical Characterization. Polarization curves were carried out in a classic three-electrode cell consisting of a silver/silver chloride reference electrode, a stainless steel counter electrode, and carbon steel specimens as a working electrode in the horizontal position, with a working area of 6.60 cm^2. The carbon steel working electrodes were ground with SiC papers to 1200-grit-finish and cleaned with ethanol in an ultrasonic bath for 5 min. After that, measurements were carried out at room temperature using a potentiostat/galvanostat (AutoLab EcoChemie PGSTAT30) equipped with NOVA 1.6 software. The scanning range was +0,250 V, −0,250 V versus OCP, the stabilization time was 30 minutes, and the scanning rate was 0.5 mV/s. The electrolyte used was 10 mM Na_2SO_4 solution at three different pH values (3, 6, and 11), without and with the addition of 2 mg/mL of loaded/encapsulated mesoporous silica nanoparticles. Measurements were carried out after 30 minutes of exposure to the different electrolytes.

3. Results and Discussion

SEM images at two different magnifications as well as a representative EDX spectrum of the synthetized mesoporous nanoparticles after the calcination step are shown in Figure 1. The iron signal comes from the iron grid used for the deposition of the nanoparticles. As can be seen, a successful synthesis of homogeneous monodisperse spherical silica nanoparticles in a diameter range of 150–200 nm has been achieved. In addition, as it was observed in the TEM (Figure 2(a)) a mesoporous structure with a pore diameter lower than 5 nm has been obtained. Similar to the case of the SEM, the Cu signal observed in the EDX spectrum comes from the grid used to deposit the nanoparticles.

Therefore, the particles were subject to the loading process with sodium phosphomolybdate. Although ideally the most convenient way of loading mesoporous silica with corrosion inhibitors is by direct incorporation during synthesis, this option has to be discarded many times due to different reasons: molecules that corrupt the formation of the mesoporous matrix, compounds that are insoluble in the synthesis solution, pore volume occupied by surfactant that is inaccessible for the storage of the inhibitor reducing the loading capacity, and so forth. The attempts to incorporate molybdate during synthesis resulted in particles of very irregular morphology and broad size distribution and loading capacity was lower. In addition, calcined silica is regarded as generally more stable offering durability in service [27]. For those reasons although the postsynthetic loading of particles after calcination requires additional steps in sample preparation, it was the methodology used.

It is known that the highest loading capacity is obtained only for a specific range of pH taking into account the tendency of molybdates to form polyanions in acid solvents [17, 28]. At very low pH the size of the polyanions is too big to infiltrate the mesopores. The molecules are stopped at the pore mouths and only these or other molecules adsorbed at the external surface are loaded. In water, where only individual MoO_4^{2-} tetrahedrae are present [29], the penetration of the mesoporous system is more likely. However, the fact that both silica and molybdate bear the same charge disfavors high loading efficiency. Only at the optimal pH are the polyanions small enough to enter the pores and the electrostatic repulsion of silica minimized (vicinity of the point of zero charge $pH_{PZC} = 2$) [30]. In our case, the selected pH was 2.3 because in a preliminary test screening the highest loading capacity was observed when the pH of the solution was adjusted to this value.

In Figure 3, both SEM and TEM images as well as a representative EDX spectrum of the mesoporous nanoparticles after the loading process with sodium phosphomolybdate are shown. As can be seen, the outward appearance has not changed but the presence of the inhibitor is confirmed by the EDX analysis.

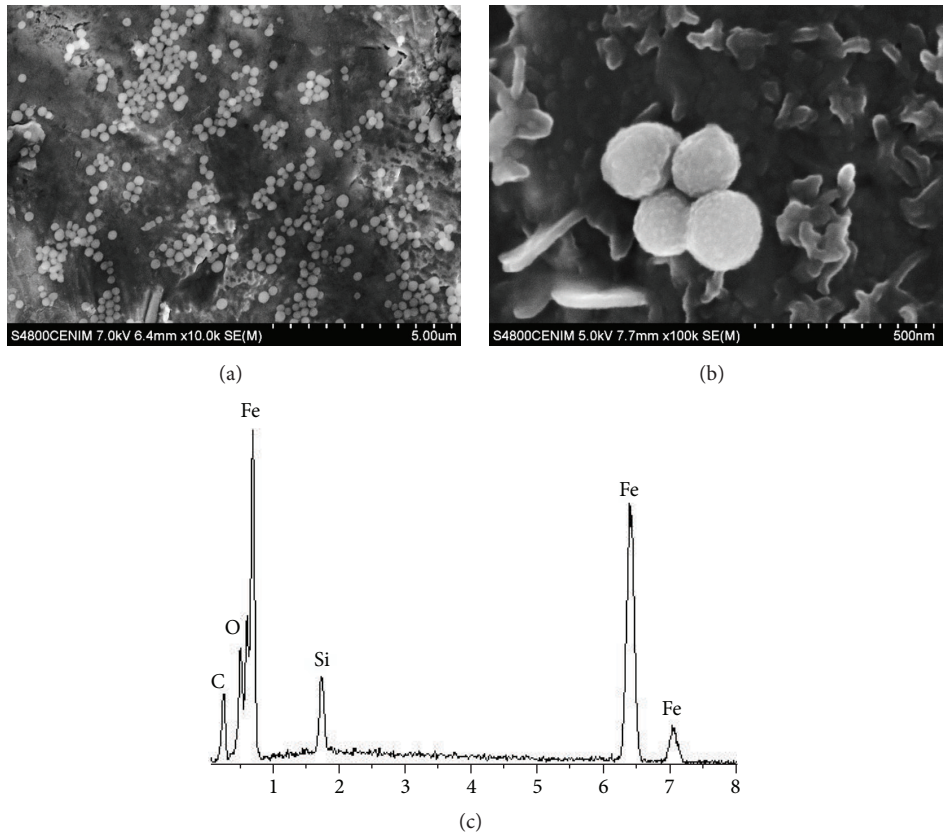

Figure 1: SEM images at two different magnifications (a) and (b) and EDX analysis (c) of the synthetized SiO_2 mesoporous nanoparticles.

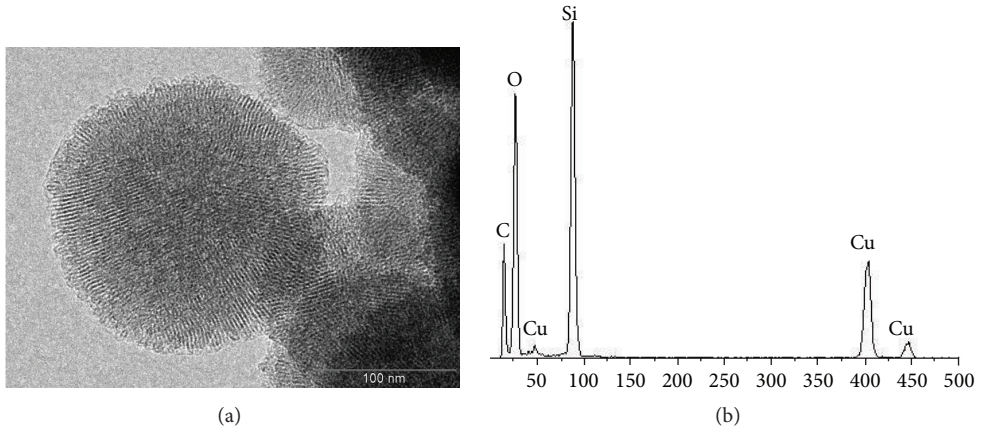

Figure 2: TEM image (a) and EDX analysis (b) of the synthetized SiO_2 mesoporous nanoparticles.

As commented before, encapsulation of the loaded nanoparticles is important for avoiding undesirable spontaneous delivery and, simultaneously, for allowing a tunable release of the inhibitor as a function of an external stimulant that interacts with the capsule. On the other hand, the presence of a suitable capsule could also help to improve the stability of the organic matrix-loaded nanoparticles system when they are incorporated with protective organic coatings. As described in Experimental Procedure, the encapsulation method tested has been the application of a layer of a positively charged polyelectrolyte, poly(diallyldimethylammonium chloride) (PDDA). The application of this type of layer can provide an intelligent release of the corrosion inhibitor, as the permeability of the polyelectrolyte assemblies can be regulated by pH, humidity, light, and so forth [21–25]. A change in pH is a more preferable trigger for corrosion protection systems since, as is well known, corrosion activity leads to local changes in

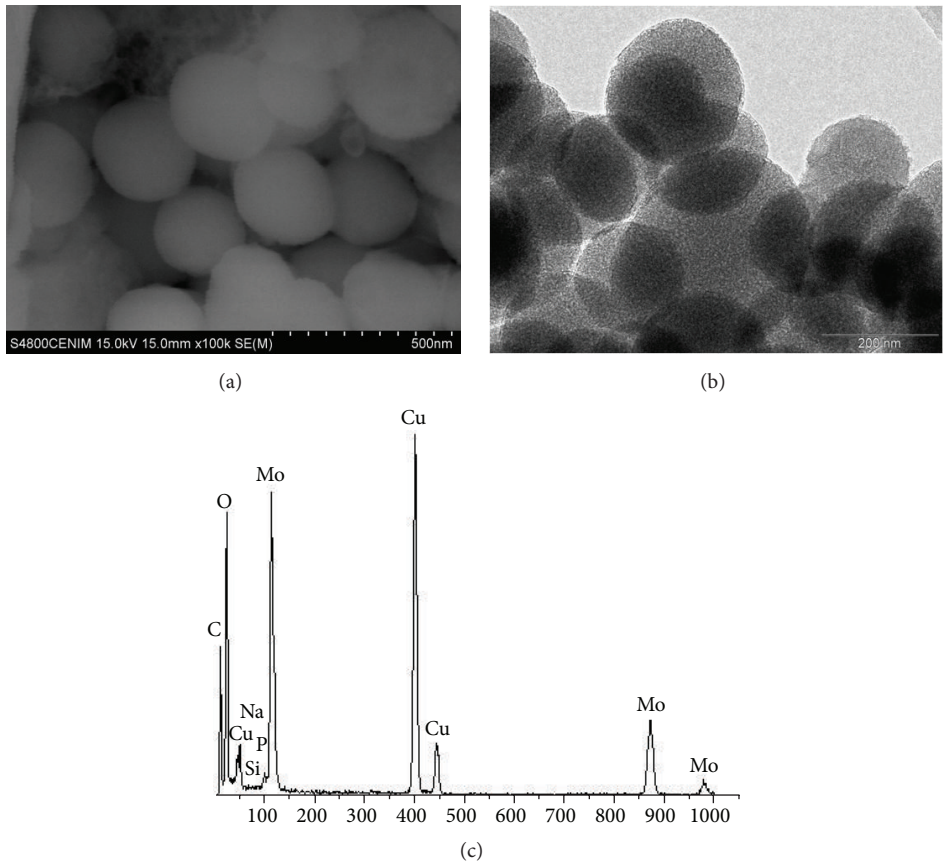

Figure 3: SEM image (a), TEM image, (b) and EDX analysis (c) of the SiO_2 mesoporous nanoparticles after loading with sodium phosphomolybdate.

pH in the cathodic and anodic areas [31]. A "smart" coating that contains polyelectrolyte reservoirs may use the corrosion reaction to release the corrosion inhibitor.

SEM and TEM images as well as a representative EDX spectrum of the loaded/encapsulated mesoporous silica nanoparticles are shown in Figure 4. As can be seen in the EDX spectrum encapsulation was also successful as can be drawn by the presence of Na and Cl. On the other hand, the presence of the capsule can be also observed at the edge of the nanoparticles in the TEM image (Figure 4(b)). The presence of Mo and P also confirms that the inhibitor has been successfully stored inside the mesoporous structure during the encapsulation process.

The characterization study has been completed by the determination of the specific surface area (S_{BET}), pore volume (V_p), and Z-potential of all produced silica nanoparticles: after being calcined, loaded, and loaded/encapsulated.

Table 1 shows the BET surface area (S_{BET} (m^2/g)), pore volume (V_p (cm^3/g)), and Z-potential (mV) obtained on the different nanoparticles. The S_{BET} and V_p values obtained after calcination are in agreement with the typical reported values of similar mesoporous silica nanoparticles [32–34]. As can be observed, the significant decrease of the BET surface area and the pore volume after loading and especially after encapsulation confirms the success of the loading and encapsulation processes. On the other hand, the change in polarity from negative to positive values in the Z-potential of the loaded/encapsulated nanoparticles definitively confirms the effectiveness of the encapsulation process based on the application of a layer of poly(diallyldimethylammonium chloride) (PDDA) as oppositively charged polyelectrolyte.

Table 1: BET/BJH and Z-potential characterization analysis.

Nanoparticles	S_{BET} (m^2/g)	V_p (cm^3/g)	Z-potential (mV)
After calcination	926.53	0.5369	−41.43
Loaded	342.11	0.2046	−53.37
Loaded/encapsulated	122.26	0.0886	51.40

As shown above, the particles have been successfully synthetized, loaded, encapsulated, and characterised by different techniques. However, it is important to quantify the loading and releasing capacity, especially as a function of external pH value, in order to validate the efficiency and possible applications of this smart and environmentally friendly alternative to the use of chromates as anticorrosive pigment in organic coatings. In this sense, Figure 5 shows the release of the inhibitor as a function of pH, measured as mg of Mo per g of nanoparticles.

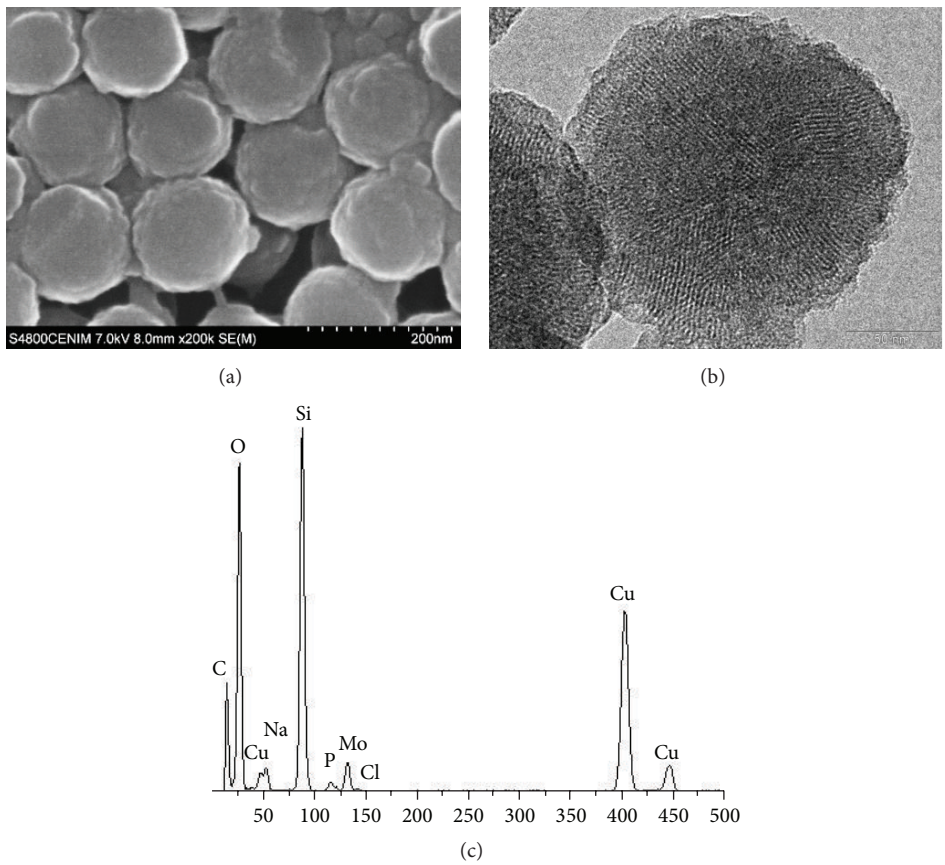

Figure 4: SEM image (a), TEM image, (b) and EDX analysis (c) of the SiO_2 mesoporous nanoparticles loaded with sodium phosphomolybdate and encapsulated by a PDDA layer.

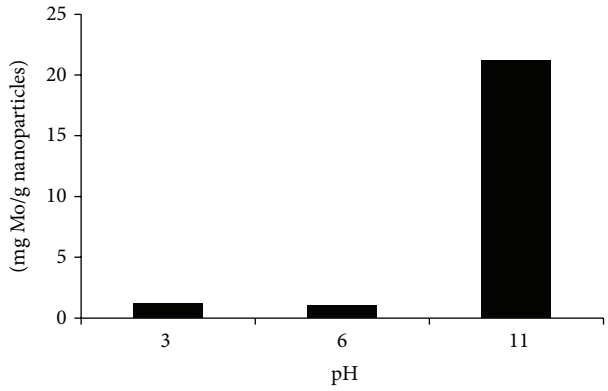

Figure 5: Inhibitor released as a function of pH, mg Mo/g nanoparticles.

As expected, the presence of the capsule avoids the release of the inhibitor at neutral and acidic pH values but allows a significant release of the inhibitor when pH > 10. At this high pH, both the capsule and the SiO_2 nanoparticles are unsteady and the inhibitor is completely released. As can be seen, the loading capacity, which is approximately the released amount of inhibitor at pH = 11, is slightly higher than 20 mg Mo/g nanoparticles.

To complete the study, the efficiency of the smart encapsulated/loaded silica nanoparticles to protect a carbon steel substrate has been studied by means of polarization curves. Figure 6 shows the polarization curves obtained on carbon steel after 30 minutes of exposure to Na_2SO_4 10 mM solution at three different pH values (3, 6, and 11), without (Figure 6(a)) and with the addition of 2 mg/mL of loaded/encapsulated mesoporous silica nanoparticles, respectively (Figure 6(b)). The current density values obtained are presented in Table 2.

As can be seen, in the absence of nanoparticles, there are no significant differences in the current as a function of pH and only a slight displacement in the E_{corr} to more negative potentials in the case of pH 3 was observed. However, with the addition of the nanoparticles the current decreases one order of magnitude in the case of pH 11 compared to the value obtained at pH 3 with nanoparticles and also one order of magnitude compared to the values obtained at all tested pH values in the case of the absence of nanoparticles, thus confirming the successful release of the inhibitor at high pH values and its protection ability.

4. Conclusions

(i) SiO_2 mesoporous nanoparticles have been successfully synthesized, loaded with an environmentally

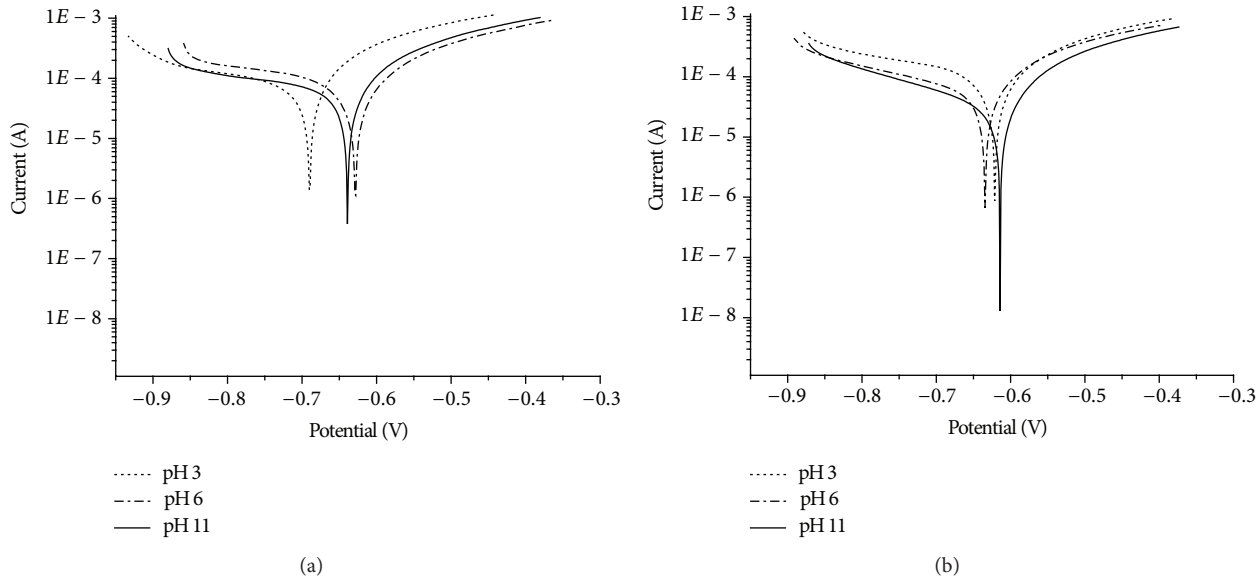

Figure 6: Polarization curves obtained on carbon steel after 30 minutes of exposure to Na_2SO_4 10 mM solution at three different pH values (3, 6, and 11) without the addition of nanoparticles (a) and with the addition of 2 mg/mL of loaded/encapsulated mesoporous silica nanoparticles (b).

Table 2: Calculated current density values obtained from the experimental polarization curves.

	pH value	Current density (μA/cm^2)
Reference (without nanoparticles)	3	113.0
	6	115.0
	11	108.4
With the addition of 2 mg/mL of nanoparticles	3	148.2
	6	83.5
	11	18.9

friendly corrosion inhibitor (sodium phosphomolybdate), and encapsulated by the deposition technology of oppositely charged polyelectrolytes.

(ii) It has been proven that at pH 11 the dissolution of the capsules is allowed, the release of the inhibitor has been verified, and the protection of carbon steel substrate has been improved.

(iii) Therefore, a smart pH-dependent nanocapsule has been developed as possible future alternative to the use of toxic chromates in organic coatings.

Conflict of Interests

The authors declare that there is no conflict of interests regarding the publication of this paper.

Acknowledgment

The authors gratefully acknowledge financial support for this work from the Ministry of Economy and Competitiveness of Spain (MAT 2011-28178).

References

[1] G. W. Walter, "A critical review of the protection of metals by paints," *Corrosion Science*, vol. 26, no. 1, pp. 27–38, 1986.

[2] H. Wang, F. Presuel, and R. G. Kelly, "Computational modeling of inhibitor release and transport from multifunctional organic coatings," *Electrochimica Acta*, vol. 49, no. 2, pp. 239–255, 2004.

[3] S. A. Katz and H. Salem, "The toxicology of chromium with respect to its chemical speciation: a review," *Journal of Applied Toxicology*, vol. 13, no. 3, pp. 217–224, 1993.

[4] ATSDR, "Toxicological profile for chromium," Tech. Rep. ATSDR/TP-88/10, Agency for Toxic Substances, US Public Health Service, 1989.

[5] S. Langard and T. Norseth, "A cohort study of bronchial carcinomas in workers producing chromate pigments," *British Journal of Industrial Medicine*, vol. 32, no. 1, pp. 62–65, 1975.

[6] International Agency for Research on Cancer, *Volume 49: Chromium, Nickel, and Welding*, International Agency for Research on Cancer, Lyon, France, 1990.

[7] Occupational Safety and Health Administration and U.S. Department of Labor, "Small entity compliance guide for the hexavalent chromium standards," OSHA 3320-10N, Occupational Safety and Health and Administration U.S. Department of Labor, 2006.

[8] D. G. Shchukin and H. Möhwald, "Self-repairing coatings containing active nanoreservoirs," *Small*, vol. 3, no. 6, pp. 926–943, 2007.

[9] E. V. Skorb, D. Fix, D. V. Andreeva, H. Möhwald, and D. G. Shchukin, "Surface-modified mesoporous SiO_2 containers for corrosion protection," *Advanced Functional Materials*, vol. 19, no. 15, pp. 2373–2379, 2009.

[10] I. A. Kartsonakis, E. P. Koumoulos, A. C. Balaskas, G. S. Pappas, C. A. Charitidis, and G. C. Kordas, "Hybrid organic-inorganic multilayer coatings including nanocontainers for corrosion protection of metal alloys," *Corrosion Science*, vol. 57, pp. 56–66, 2012.

[11] C. Ávila-Gonzalez, R. Cruz-Silva, C. Menchaca, S. Sepulveda-Guzman, and J. Uruchurtu, "Use of silica tubes as nanocontainers for corrosion inhibitor storage," *Journal of Nanotechnology*, vol. 2011, Article ID 461313, 9 pages, 2011.

[12] E. Abdullayev, R. Price, D. Shchukin, and Y. Lvov, "Hallosyte tubes as nanocontainers for anticorrosion coating with benzotriazole," *Applied Materials Science*, vol. 1, no. 7, pp. 1437–1443, 2009.

[13] D. G. Shchukin, M. Zheludkevich, K. Yasakau, S. Lamaka, M. G. S. Ferreira, and H. Möhwald, "Nanocontainers for self-healing corrosion protection," *Advanced Materials*, vol. 18, pp. 1672–1678, 2006.

[14] D. G. Shchukin and H. Möhwald, "Smart nanocontainers as depot media for feedback active coatings," *Chemical Communications*, vol. 47, no. 31, pp. 8730–8739, 2011.

[15] T. Chen and J. J. Fu, "pH-responsive nanovalves based on hollow mesoporous silica spheres for controlled release of corrosion inhibitor," *Nanotechnology*, vol. 23, no. 23, Article ID 235605, 2012.

[16] A. Kumar, L. D. Stephenson, and J. N. Murray, "Self-healing coatings for steel," *Progress in Organic Coatings*, vol. 55, no. 3, pp. 244–253, 2006.

[17] M. Walczak, *Release studies on mesoporous microcapsules for new corrosion protection systems [Ph.D. thesis]*, Rühr-University, Bochum, Germany, 2007.

[18] R. K. Iller, *The Chemistry of Silica: Solubility, Polymerization, Colloid and Surface Properties and Biochemistry of Silica*, Wiley, 1979.

[19] G. Decher, J. D. Hong, and J. Schmitt, "Buildup of ultrathin multilayer films by a self-assembly process: III. Consecutively alternating adsorption of anionic and cationic polyelectrolytes on charged surfaces," *Thin Solid Films*, vol. 210-211, no. 2, pp. 831–835, 1992.

[20] G. Decher, "Fuzzy nanoassemblies: toward layered polymeric multicomposites," *Science*, vol. 277, no. 5330, pp. 1232–1237, 1997.

[21] K. Glinel, M. Prevot, R. Krustev, G. B. Sukhorukov, A. M. Jonas, and H. Möhwald, "Control of the water permeability of polyelectrolyte multilayers by deposition of charged paraffin particles," *Langmuir*, vol. 20, no. 12, pp. 4898–4902, 2004.

[22] Z. H. Lu, M. D. Prouty, Z. H. Quo, V. O. Golub, C. S. S. R. Kumar, and Y. M. Lvov, "Magnetic switch of permeability for polyelectrolyte microcapsules embedded with Co@Aunanoparticles," *Langmuir*, vol. 21, no. 5, pp. 2042–2050, 2005.

[23] D. G. Shchukin and G. B. Sukhorukov, "Nanoparticle synthesis in engineered organic nanoscale reactors," *Advanced Materials*, vol. 16, no. 8, pp. 671–682, 2004.

[24] G. B. Sukhorukov, "Novel methods to study interfacial layers," in *Studies in Interface Science*, D. Mobius and R. Miller, Eds., vol. 11, p. 38, Elsevier, Amsterdam, The Netherlands, 2001.

[25] Y. Lvov, A. A. Antipov, A. Mamedov, H. Möhwald, and G. B. Sukhorukov, "Urease encapsulation in nanoorganized microshells," *Nano Letters*, vol. 1, no. 3, pp. 125–128, 2001.

[26] Y. Yamada and K. Yano, "Synthesis of monodispersed supermicroporous/mesoporous silica spheres with diameters in the low submicron range," *Microporous and Mesoporous Materials*, vol. 93, no. 1–3, pp. 190–198, 2006.

[27] F. Kleitz, W. Schmidt, and F. Schüth, "Calcination behavior of different surfactant-templated mesostructured silica materials," *Microporous and Mesoporous Materials*, vol. 65, no. 1, pp. 1–29, 2003.

[28] N. N. Greenwood and A. Earnshaw, "Isopolymetallates," in *Chemistry of the Elements*, chapter 23.3.2, Pergamon Press, 1986.

[29] C. E. Easterly, D. M. Hercules, and M. Houalla, "Electrospray-ionization time-of-flight mass spectrometry: pH-dependence of phosphomolybdate species," *Applied Spectroscopy*, vol. 55, no. 12, pp. 1671–1675, 2001.

[30] G. A. Parks, "The isoelectric points of solid oxides, solid hydroxides, and aqueous hydroxo complex systems," *Chemical Reviews*, vol. 65, no. 2, pp. 177–198, 1965.

[31] L. S. Kasten, J. T. Grant, N. Grebasch, N. Voevodin, F. E. Arnold, and M. S. Donley, "An XPS study of cerium dopants in sol-gel coatings for aluminum 2024-T3," *Surface and Coatings Technology*, vol. 140, no. 1, pp. 11–15, 2001.

[32] D. Borisova, H. Möhwald, and D. G. Shchukin, "Mesoporous silica nanoparticles for active corrosion protection," *ACS Nano*, vol. 5, no. 3, pp. 1939–1946, 2011.

[33] X. Huang, N. P. Young, and H. E. Townley, "Characterization and comparison of mesoporous silica particles for optimized drug delivery," *Nanomaterials and Nanotechnology*, vol. 4, article 2, 2014.

[34] I. I. Slowing, J.-L. Vivero-Escoto, C.-W. Wu, and V. S.-Y. Lin, "Mesoporous silica nanoparticles as controlled release drug delivery and gene transfection carriers," *Advanced Drug Delivery Reviews*, vol. 60, no. 11, pp. 1278–1288, 2008.